

A COMPACT ON-BOARD AIRCRAFT SECTORIAL ANTENNA

Patrice Brachat⁽¹⁾, Raymond Bills⁽¹⁾, Philippe Ratajczak⁽¹⁾, Christian Sabatier⁽¹⁾, Eric Seguenot⁽¹⁾, Patrice Bongibault⁽²⁾, Joel Mailloux⁽²⁾, Thomas Vitte⁽²⁾, Yannick Beniguel⁽³⁾

⁽¹⁾FRANCE TELECOM R&D, Fort de la tête de chien, 06320 La Turbie, FRANCE.

Email: patrice.brachat@orange-ft.com, raymond.bills@orange-ft.com, philippe.ratajczak@orange-ft.com, chris.sabatier@orange-ft.com, eric.seguenot@orange-ft.com

⁽²⁾EADS Defence and Security Systems SA, Defence Electronics Communications and Data Link Systems, Rue J.P. Timbaud, BP 26, 78063 Montigny Le Bretonneux Cedex, FRANCE.

Email: patrice.bongibault@eads.com, joel.mailloux@eads.com, thomas.vitte@eads.com

⁽³⁾IEEA, 13, Promenade Paul Doumer, 92400 Courbevoie, FRANCE.

Email: beniguel@club-internet.fr

ABSTRACT

Results of a compact sectorial antenna to be used under an aircraft are presented in this paper. The objective is to simulate an airborne node authorizing the communications between ground gateways.

1. INTRODUCTION

EADS Defence and Security Systems was selected by the DGA (French DoD) to develop a new communication system called ACN (Airborne Communication System). The ACN provides a communication service characterized by very high capacity and very high coverage area on easy and quickly deployable gateways, without any infrastructures. The ground gateways communicate through an airborne node, set up in an aircraft at an altitude of 33000 ft. Considering the specific constraints due to the integration under an aircraft (low weight and size, 33000 ft. altitude environment) to the large coverage area (50 km radius, that means 170 degrees aperture), the circular polarization, the need to get the same power in the whole area and the need to get a low dispersion (< 1 dB) of the patterns in the wide frequency band (14.47-15.16 GHz), this led to develop a totally new compact antenna with profiled reflectors. This antenna is presented in the article.

2. DESCRIPTION OF THE ANTENNA

A schematic view of the antenna is presented in figure 1. It is made of a septum polarizer computed with SR3D software [1] and an antenna designed with SRSR software tool [2] which is composed of a horn and two shaped reflectors. The sub-reflector is positioned near the aperture of the feed (a few centimeters). A glued dielectric rod is used between the sub-reflector and the

feed to maintain the assembly. The circular septum polarizer (axial ratio < 0.5 dB for LHCP and RHCP) is integrated in the main reflector of the antenna. Ports for the two modes are SMA 3.5 mm connectors.

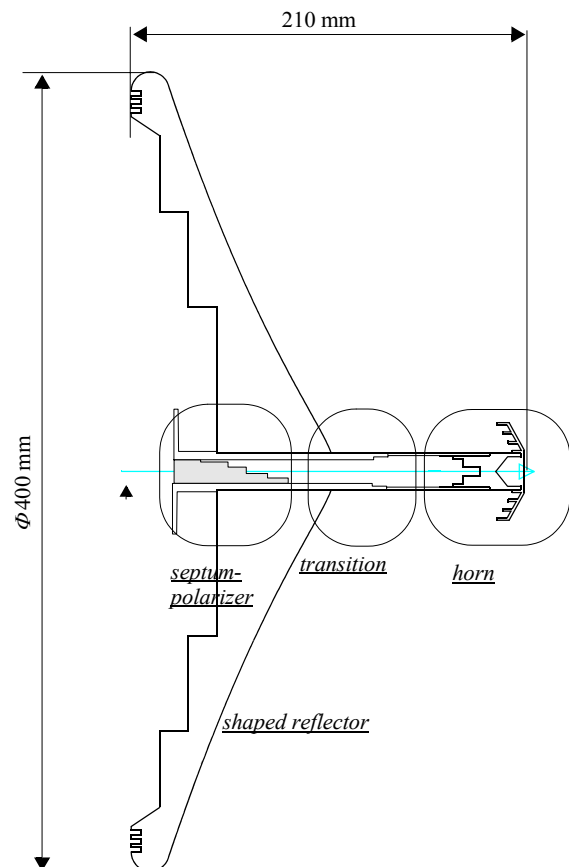


Figure 1 : Schematic view of the complete antenna.

The diameter of the antenna is 40 cm and its height is 21 cm.

3. RESULTS

The antenna was measured in our anechoic chamber (spherical near fields technique) at FTR&D La Turbie. Four cuts in circular polarization were registered for each frequency.

3.1. Far fields patterns - RHCP mode

The far fields patterns for the RHCP mode at 14.6 GHz and 15.05 GHz are plotted in figure 2 and 3 respectively.

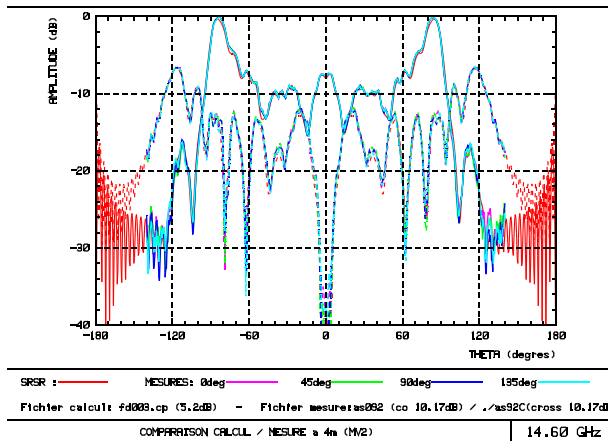


Figure 2 : Computed cut (red) and specific measured cuts at 14.6 GHz for the RHCP mode.

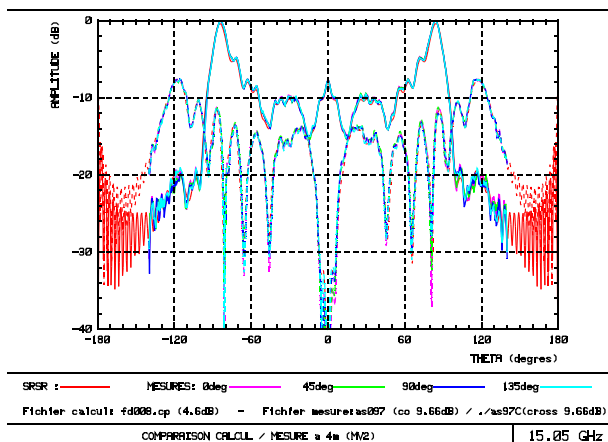


Figure 3 : Computed cut (red) and specific measured cuts at 15.05 GHz for the RHCP mode.

The correlation between simulated and measured patterns is excellent.

3.2. Variation of the far fields patterns for the RHCP mode

The frequency band is separated in two bands (14.47 - 14.72 GHz and 14.93 - 15.16 GHz) to draw the

dispersion of the far fields patterns. This dispersion is shown in figure 4. A very low variation (< 1dB) of the co-polarization up to 100 degrees is obtained.

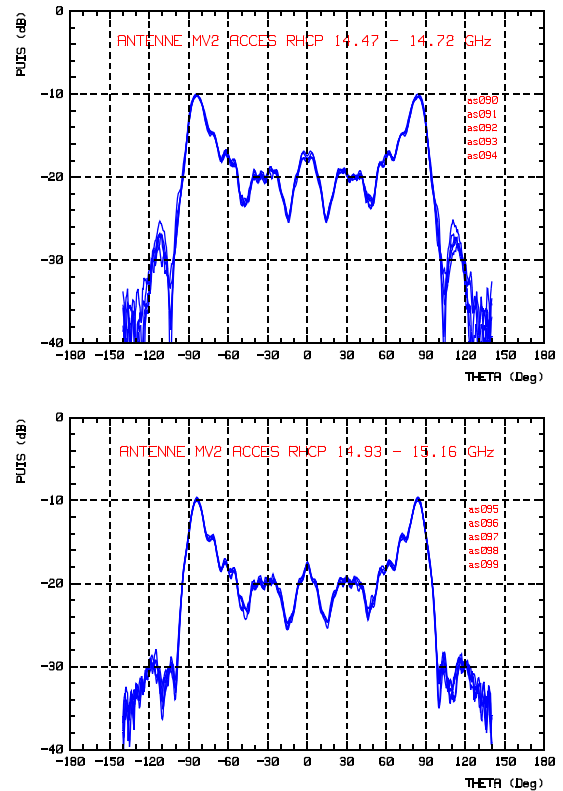


Figure 4 : Frequency dispersion of the measured far fields patterns for the RHCP mode.

3.3. Far fields patterns - LHCP mode

Results of the far fields patterns for the LHCP mode are very closed to the results for the RHCP mode. They are presented in figure 5 for the frequency 14.6 GHz and in

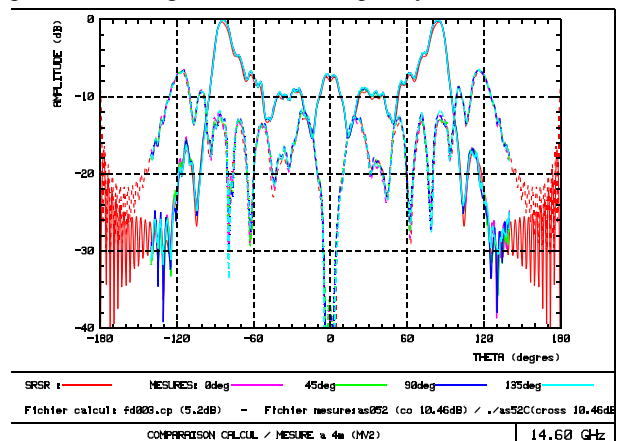


Figure 5 : Computed cut (red) and specific measured cuts at 14.6 GHz for the LHCP mode.

figure 6 for the frequency 15.05 GHz.

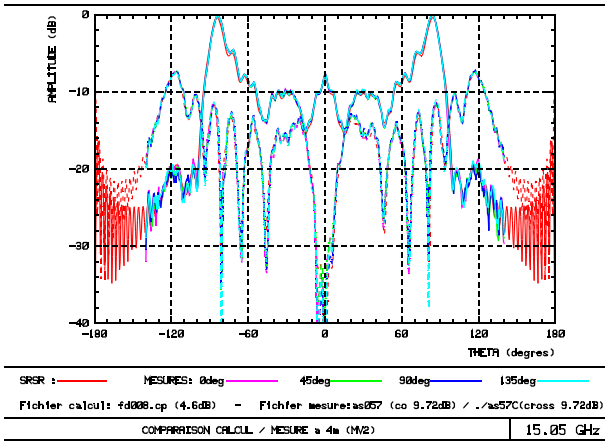


Figure 6 : Computed cut (red) and specific measured cuts at 15.05 GHz for the LHCP mode.

Excellent agreement is obtained between the computed values and the measured values on the whole frequency band.

3.4. Variation of the far fields patterns for the LHCP mode

The dispersion is given in figure 7. Similar for the RHCP

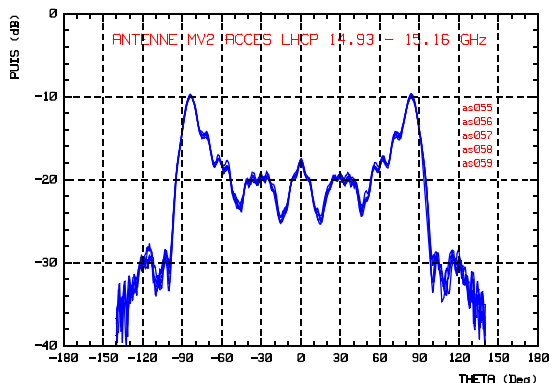
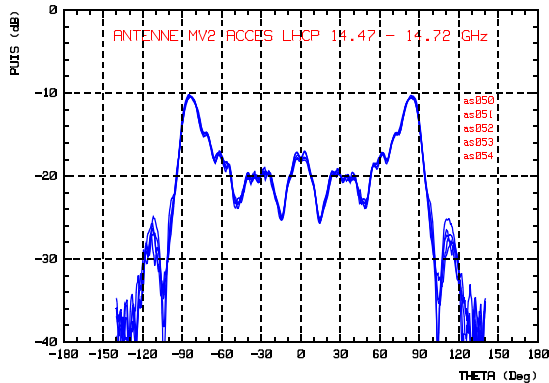


Figure 7 : Frequency dispersion of the measured far fields patterns for the LHCP mode.

mode, a very low variation (< 1dB) of the co-

polarization up to 100 degrees is obtained for the LHCP mode.

3.5. Gain

The measurement of this parameter is realized by a comparison with a reference antenna at the maximum of the far fields (theta = -84 degrees, phi = 0 degree). The gain is always higher than 6 dBi on all the frequency band and for both circular polarizations (see figure 8)

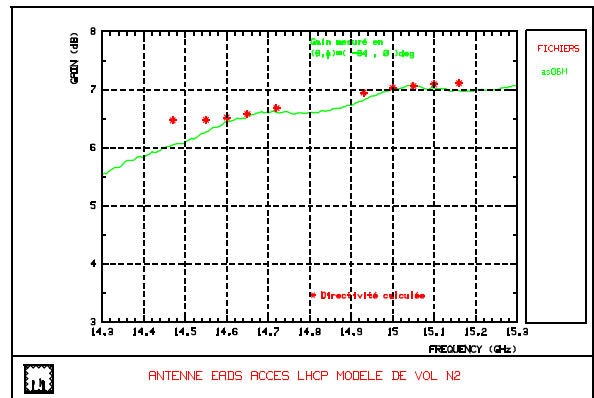
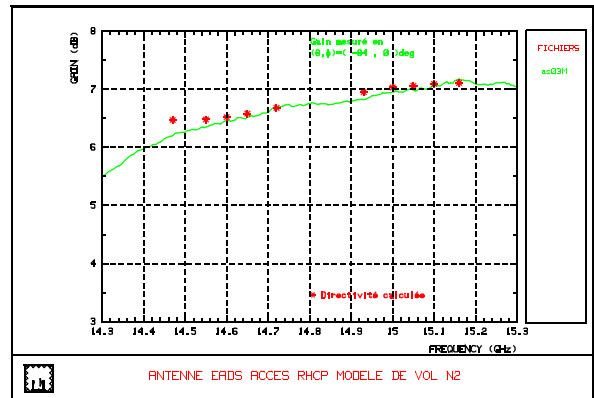


Figure 8 : Gain for the RHCP and LHCP modes.

with similar levels for the two ports. Stars symbols on these plots represent the directivities computed by integrating the far fields patterns given by [2]. Losses are lower than 0.3 dB which is low although there is a glued dielectric rod for maintaining the sub-reflector.

3.6. S parameters

S parameters are registered with a network analyzer. The VSWR is better than 1.10 for both ports and in all the frequency band (14.47 - 15.16 GHz). Isolation between the RHCP port and the LHCP port is better than 17 dB.

4. UTD ASYMPTOTIC TECHNIQUE USED FOR ANTENNA IMPLEMENTATION ON ELECTRICALLY LARGE STRUCTURES

The implementation of antennas in a complex environment still remains a problem when high frequencies are considered. The Uniform geometrical Theory of Diffraction (UTD) is one of the most convenient techniques to solve this problem [3]. Compared with other methods, the UTD has some interesting advantages. It is an efficient tool to understand the phenomenology because the global field results from localized contributors. In addition, the computational time is reduced. It is frequency independent and enables the software to handle electrically large structures.

4.1. Structure Geometry

One simple and efficient way to describe the structure is to use NURBS curves and surfaces, which are imported from common CAD formats, like for example IGES or CATIA. NURBS is a parametric representation of a 3D curve or surface. It allows an accurate description of any arbitrary shape. The surface curvature is easily derived. It is an important parameter for UTD coefficients computation. Figure 9 presents the structure described with NURBS. Very few NURBS surfaces were needed to describe the geometry.

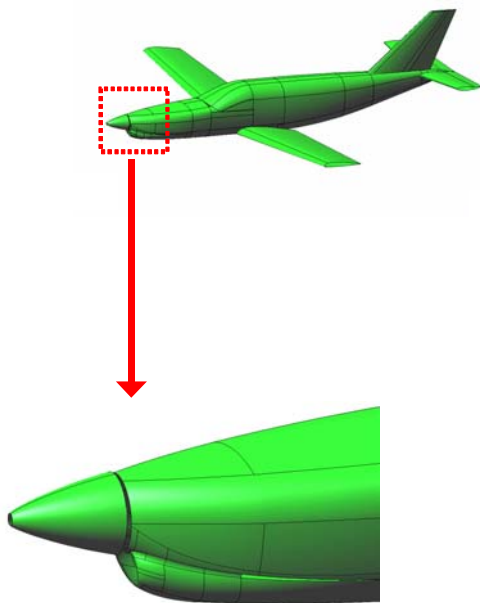


Figure 9 : The aircraft described with NURBS surfaces and curves.

4.2. Application: Antenna implementation

The UTD calculation is performed using a ray tracing technique. Once the rays are traced, the UTD coefficients are applied to compute the electric field. Several outputs can be provided like near field maps or radiation patterns. These values are important parameters for antenna design and may be highly dependent on the antenna environment.

As the computation speed is very high, many iterations can be done in a limited time. This feature makes the technique very suitable for optimization routines. The input of the problem is the position of the antenna. The cost function is the difference between the parameter to reach and the computed value of this parameter. In this case, the cost function is the difference between the free space radiation pattern and the computed radiation pattern and the aim is minimizing the influence of the environment.

An interesting class of optimization methods is the genetic algorithms. There is usually very few information on the cost function. In addition, this function may have several local extrema. The genetic algorithms are able to manage this situation. This technique was used to obtain the result presented in figure 10. It shows the modified pattern considering the

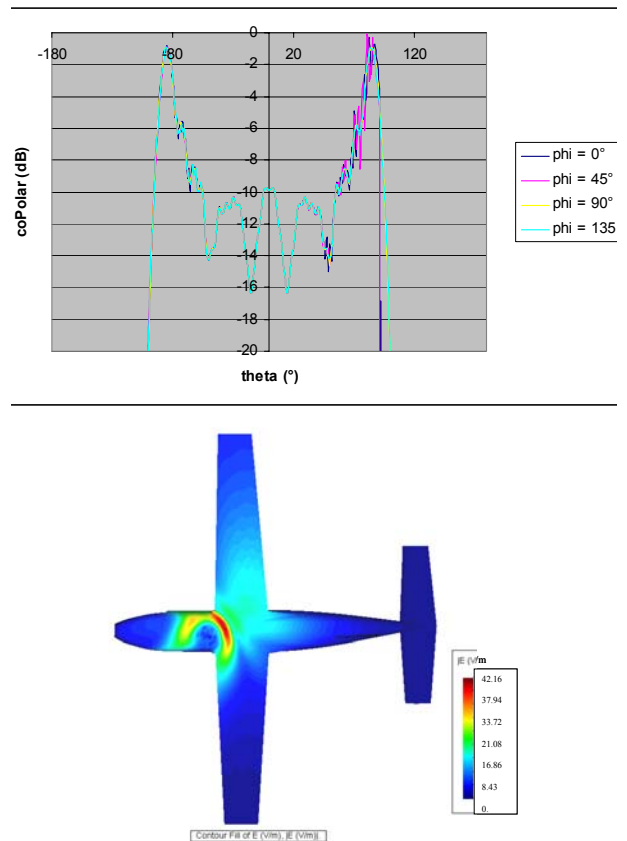


Figure 10 : Modified far fields patterns of the antenna and highest values of the fields below the aircraft.

interaction with the plane for the best antenna location found by the genetic algorithm and the electric field below the plane.

The highest values of the field were localized at the antenna vicinity. Absorbing material was placed in this area in order to decrease its value.

5. CONCLUSION

Photos of the antenna and of the breadboard septum polarizer are presented in figure 11.

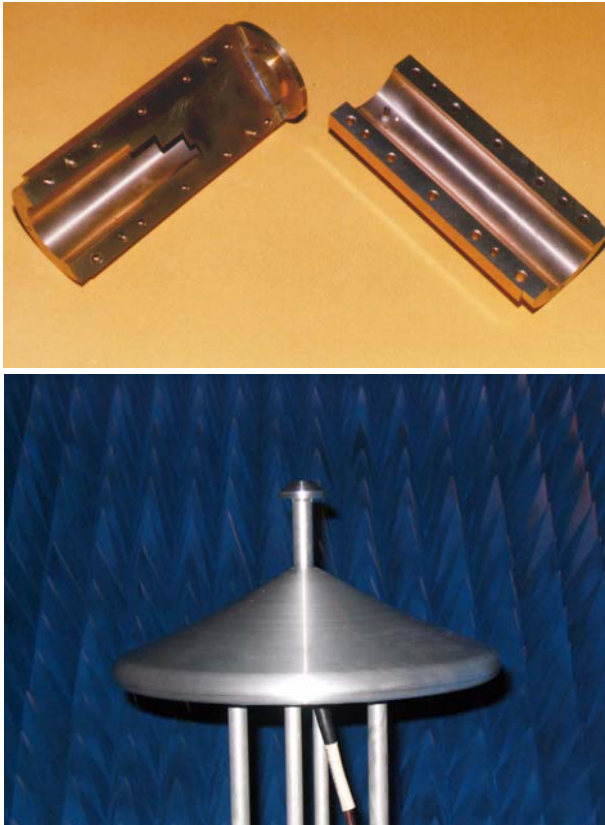


Figure 11 : Photos of the breadboard septum and the antenna.

All measurements of the antenna were compliant with the required specifications. Mechanical tests were performed and passed with success. Two flight models based on this antenna were manufactured. All results of these FMs are completely similar to the results presented in this paper.

The position of the antenna below the aircraft was optimized with a genetic algorithm associated with an asymptotic analysis. A photo of the antenna set below the aircraft is shown in figure 12. A radome is mounted before the take-off (figure 13).

REFERENCES

- [1] PRATAJCZAK, P.BRACHAT and C.DEDEBAN, "Modeling of arbitrarily radiating elements using the CAD tool SR3D", IEEE /AP-S International Symposium and USNC/URSI Radio Science Meeting, Montreal, 1997.
- [2] A.BERTHON, R.BILLS, "Integral Equations Analysis of Radiating Structures of Revolution". IEEE Trans. Antennas and Propagation, Vol. AP-37, no. 2, pp. 159-170, Feb. 1989.
- [3] J.P.ADAM, Y.BENIGUEL, "UTD asymptotic code used for antenna implementation on electric large structures", Proceedings 11e International Symposium on Antennas Technology and Applied Electromagnetics, St Malo, June 15-17, 2005.



Figure 12 :Antenna below the aircraft.



Figure 13 : Aircraft before take-off.